

Low temperature thermodynamical properties of the organic chain conductor (TMTSF)₂AsF₆

J.-C. Lasjaunias^{1,a}, K. Biljaković^{1,2}, D. Starešinić², P. Monceau¹, S. Takasaki³, J. Yamada³, S.-I. Nakatsuji³, and H. Anzai³

¹ Centre de Recherches sur les Très Basses Températures^b, B.P. 166, 38042 Grenoble Cedex 9, France

² Institute of Physics, POB 304, HR 10001 Zagreb, Croatia

³ Department of Material Science, Faculty of Science, Himeji Institute of Technology, Kamigohri, Hyogo 678-12, Japan

Received: 17 March 1998 / Revised: 27 July 1998 / Accepted: 22 September 1998

Abstract. We report on specific heat measurements of the quasi-one-dimensional organic salt (TMTSF)₂AsF₆ in its spin density wave state between 75 mK and 7 K. Similarly to (TMTSF)₂PF₆, we find discontinuities in the lattice contribution at 1.9 K and 3.5 K ascribed to sub-spin density wave phases. Time-dependent effects due to dynamics of low-energy excitations in metastable states occur only below 0.2 K which yields an activation energy for the equilibrium energy relaxation process of 0.34 K, 4–5 times smaller than found for (TMTSF)₂PF₆. Finally the reduction of the low-energy excitations contribution to the specific heat in comparison to PF₆ reveals an intermediate cubic-like regime between 0.25 and 0.5 K that we tentatively describe as the phason contribution of the incommensurate spin density wave modulation.

PACS. 75.30.Fv Spin density wave – 05.70.Ln Non-equilibrium thermodynamics, irreversible processes

1 Introduction

Conducting organic Bechgaard salts of general formula (TMTSF)₂X (TMTSF: tetramethyltetraselenafulvalene, X: PF₆, AsF₆, ClO₄, NO₃ ...) are quasi one-dimensional model systems for the study of broken symmetry ground states. These salts display a great variety of properties such as spin density wave (SDW), superconductivity, anion ordering, field induced SDW, quantum Hall effect, ... [1], which are the consequence of the highly anisotropic electronic structure of these compounds.

NMR studies have revealed that the SDW modulation is incommensurate with the lattice [2]. Such incommensurate density waves (IDW) exhibit spectacular collective transport properties beyond a finite electric threshold field which depins the SDW from impurities [3]. Due to the randomness and disorder, resulting from interaction between the SDW phase and randomly distributed impurities, the SDW ground state exists in many metastable states. Consequently, many electrical and dielectric properties are characterized by a “glassy” behaviour. Low temperature thermodynamical measurements give especially a representative manifestation of these metastable states. For a broad variety of charge (CDW) and spin density waves, we have found that additional excitations to regular phonons contribute to the specific heat, C_p , below 1 K

[4,5]. In the same temperature range the non-exponential enthalpy relaxation with “aging” effects prove the non-linearity of the specific heat and reveal the broad distribution of relaxation times for recovering the thermodynamical equilibrium. These properties have been reported both for a I-CDW compound (TaS₃) [6] and for a I-SDW ((TMTSF)₂PF₆) [7,8].

In the modulated magnetic phase of (TMTSF)₂PF₆, below the SDW phase transition at $T_c = 12.1$ K, sub-SDW phases have been detected at 3.5 K and 1.9 K by measurements of the spin-lattice relaxation rate T_1^{-1} [9]. Similar experiments on (TMTSF)₂AsF₆ [10] have also shown a structural change around 3 K. This underlying cascade of instabilities in (TMTSF)₂PF₆ was also observed in our calorimetric measurements [11,12]. In view of the pronounced similarity of the discontinuity around 3.5 K with the kinetic properties of freezing in supercooled liquids, we have described this anomaly as a glassy-like transition. In this context, the jump in specific heat represents the freezing-in of the configurational degrees of freedom of the supercooled liquid beyond the experimental time scale. Comparison of the estimated configurational entropy with the electronic entropy has raised the question of a possible electron-phonon interaction in the SDW stabilization. In fact, $2k_F$ satellite reflections have been recently detected [13] from X-ray diffuse scattering measurements, indicating a mixed CDW-SDW ground state in (TMTSF)₂PF₆.

^a e-mail: lasjau@labs.polycnrs-gre.fr

^b Associé à l'Université Joseph Fourier, CNRS.

Measurements of the low-frequency dielectric susceptibility have shown a critical slowing down around 2 K of the dielectric relaxation in $(\text{TMTSF})_2\text{PF}_6$ [14]. Microwave response reveals also small changes in the dielectric constant and conductivity at 3.5 K and 1.9 K in $(\text{TMTSF})_2\text{PF}_6$ [15a], even more pronounced in $(\text{TMTSF})_2\text{AsF}_6$ [15b]. The magnetic field dependence of these sub-phase transitions in the microwave response has also been measured [15].

The magnetoresistance of these Bechgaard salts exhibit rapid oscillations which may originate from a Fermi surface reconstruction due to the SDW formation. In $(\text{TMTSF})_2\text{PF}_6$ [16], $(\text{TMTSF})_2\text{ClO}_4$ [17] and $(\text{TMTSF})_2\text{AsF}_6$ [18], the rapid oscillation amplitude has a sharp peak around 3 K, associated with a maximum of the normalized magnetoresistance. Magnetic torque measurements also show a broad maximum around 3 K [16–18].

Finally the collective transport properties in the case of $(\text{TMTSF})_2\text{AsF}_6$ are modified in the same temperature range: the threshold electric field sharply increases for $T < 3$ K, suggesting a change in the pinning mechanism [19] and the non-linear conductivity due to the SDW sliding has been shown to decrease below 3 K [20].

In order to get additional outlines of these SDW sub-phase transitions and low-temperature dynamics of SDW-excitations, we have investigated the thermodynamic properties of $(\text{TMTSF})_2\text{AsF}_6$ (in short AsF_6) in the temperature range 75 mK to 7.5 K, in close comparison to our previous studies of $(\text{TMTSF})_2\text{PF}_6$ (in short PF_6).

The main results of this study are the following:

- (i) Between 0.5 and 7.5 K, the specific heat of AsF_6 compound is very similar to that one of PF_6 with discontinuities in the lattice contribution at 1.9 K (a tiny feature) and at 3.5 K and with time-dependence effects demonstrated by the different experimental time-spans;
- (ii) In the very-low temperature region, below 0.5 K, C_p for AsF_6 is considerably smaller than for PF_6 , what we ascribe to a large reduction of the low-energy excitations (LEE) contribution. This property is confirmed by the shift at lower T (in comparison to PF_6) of the slow dynamics of the metastable LEE, which is characterized by a much lower activation energy for the equilibrium relaxation process;
- (iii) The drastic reduction of LEE reveals a new behaviour, as an intermediate cubic-like regime between 0.25 and 0.5 K, that we tentatively ascribed to the phason contribution of the incommensurate SDW modulation.

2 Experimental

Crystals of $(\text{TMTSF})_2\text{AsF}_6$ were prepared with usual procedures [21]. Specific heat was measured between 0.075 K and 7.5 K by a transient heat pulse method in a dilution refrigerator as we had already done under similar conditions with different 1D materials [8,11].

The sample in the form of a great number of needles with a weight of 92 mg was smoothly pressed between

two large silicon plates with the use of 7 mg of Apiezon *N* grease. The ratio of heat capacity of the addenda to the total specific heat increases from $\sim 30\%$ at $T = 5\text{--}7$ K to 45% at $T = 1$ K and reaches 70–75% at $T \simeq 0.1\text{--}0.3$ K (due to the rapid decrease of C_p – almost like T^3 – down to 0.2 K). Duration of heat pulses was between 0.2 s ($T \sim 0.1$ K) and 1 s ($T \sim 7$ K). Thermal transients in response to heat pulses were not a simple exponential. As previously we adopt the convention to define C_p from the initial part of transient, that means a minimum value for the time-dependent specific heat [22]. Similarly to the case of PF_6 , we can define a “short-time scale” value by the initial decay of the transient, or by the method of total integration of the heat release relaxed through the thermal link [8]. However, in the case of AsF_6 for the temperatures $T > 3$ K, the thermal transients can be described with two exponentials. The results obtained by either total integration or long-time scale estimation of relaxation time merge together at 6 K. On the other side, for $T < 0.25$ K, when the heat relaxation progressively deviates from exponential, C_p becomes strongly time-dependent.

In the following we will compare our present specific heat data of AsF_6 with previous measurements performed on PF_6 from two different batches [8,11] and on a sulphur analog of Bechgaard salts, namely $(\text{TMTTF})_2\text{Br}$ (in short Br) [23]. The experimental conditions for thermal diffusivity of the present AsF_6 sample assembly are rather similar to those in the PF_6 [8] and Br cases.

3 “Short-time scale” specific heat

We first discuss data in response to the heat pulse. As explained above, C_p is defined by the initial exponential decrease of the transient. Raw C_p data obtained in this way are reported in Figure 1 in a C/T^3 vs. T and in Figure 2 in a log C -log T diagram, and compared to the data of PF_6 [11], determined in the same way (note that in the case of PF_6 , the transients remain exactly exponential in the high T -range, from about 1 K up to 7 K). Whereas the $C_p(T)$ variations are qualitatively and quantitatively similar in the T -range from 0.5 to 7 K, a striking difference occurs below 0.5 K. In the case of PF_6 , C_p goes through a smooth minimum around 0.35 K on decreasing T and thereafter tends asymptotically to a low-temperature limit T^{-2} regime; for AsF_6 C_p follows a cubic variation down to 0.25 K, which rapidly turns to a T^{-2} regime actually obeyed between 100 and 75 mK.

In the following, we intend to discuss successively the C_p behaviour in three different T -ranges, a, b, c, as indicated in Figure 1.

a) $T \leq 0.25$ K

In this T -range, C_p deviates progressively from the cubic-like regime existing up to 0.5 K. In first approximation, this deviation can be accounted for by an hyperfine T^{-2} term. However, we will show from the comparison of the amplitude of this term to the much larger ones measured in the family compounds Br [23] and PF_6 [8], that a nuclear hyperfine origin, either electric quadrupolar

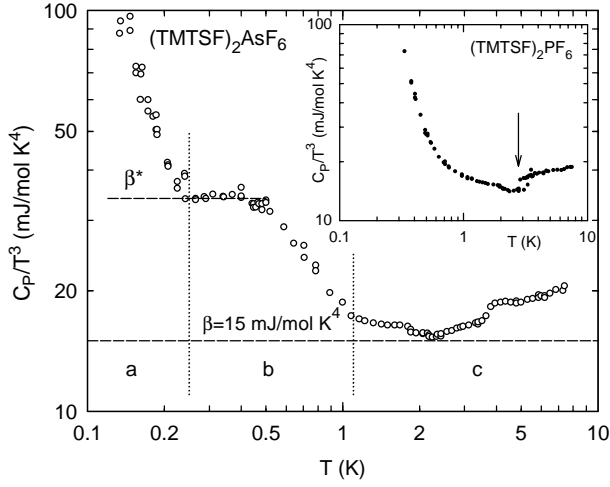


Fig. 1. The specific heat of $(\text{TMTSF})_2\text{AsF}_6$ defined on the short-time scale, divided by T^3 , between 0.15 and 7.5 K. At variance to $(\text{TMTSF})_2\text{PF}_6$ (in the inset), C_p shows an intermediate cubic regime between 0.25 and 0.5 K, whereas discontinuities at 1.9 K and 3.5 K are common to both systems. The arrow at $T = 3$ K for PF_6 indicates the onset of hysteretic phenomena ascribed to a glassy-like transition [11,12]. The horizontal dashed line $\beta = 15$ mJ/mol K^4 is the estimation of the regular phonon background, similar to PF_6 .

or magnetic, which was suggested for PF_6 [8], but already questionable for Br [23], has to be ruled out.

b) $0.25 \text{ K} \leq T \leq 1 \text{ K}$

This T -range is characterized by a smooth change between two cubic regimes (Fig. 1). Two alternative origins will be discussed: either a phonon origin or more plausibly a SDW phason contribution to C_p , as previously worked out for CDW systems [24].

c) $1 \text{ K} \leq T \leq 7 \text{ K}$

In this T -range, C_p varies almost like βT^3 , but in two successive regimes; the two being separated by a knee at $T \simeq 3.5$ K, exactly the same T where a more characteristic anomaly was detected in PF_6 , that we have ascribed to a glassy-like transition [12] (see the arrow in inset of Fig. 1). In this whole T -range, we will show that the amplitude of these quasi-cubic regimes is sensitive to the methods of measurements, essentially to the duration of the heat-delivery (supply) to the sample. We suppose that these time-dependence effects are related to the metastable character of the SDW in the vicinity of the glassy-like transition around 3 K.

3.1 Hyperfine contribution and a possible regular LEE contribution ($75 \text{ mK} \leq T \leq 250 \text{ mK}$)

In first approximation, taking into account the large uncertainty of the data between 0.1 and 0.25 K, where the amount of addenda contribution reaches 70 to 75% of the total heat capacity, it is possible to analyze C_p between 75 mK and 0.5 K as:

$$C_p = \beta^* T^3 + C_h T^{-2} \quad (1)$$

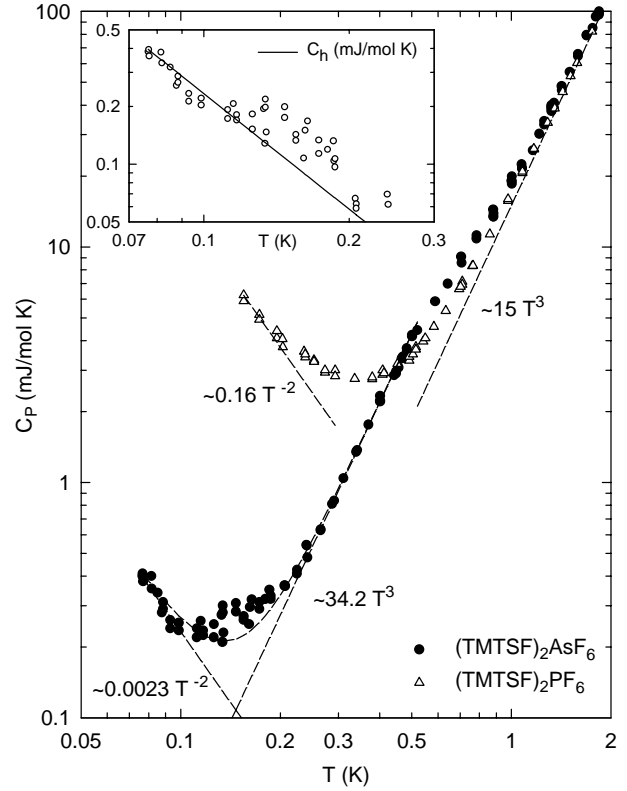


Fig. 2. The specific heat of $(\text{TMTSF})_2\text{AsF}_6$, always defined on the short-time scale, reported below 2 K in a log-log plot and directly compared to that of $(\text{TMTSF})_2\text{PF}_6$ [11]. The strong reduction of the LEE contribution in comparison to PF_6 , as evidenced by the reduction of the hyperfine T^{-2} term by a factor of 70, reveals the intermediate cubic regime ($\beta^* = 34.2$ mJ/mol K^4), that we interpret as a phason-mode contribution. In the inset is reported the difference between the total C_p of AsF_6 and the $\beta^* T^3$ term, which defines the LEE contribution. Below 0.13 K, it is well-defined by an hyperfine regime: $C_h T^{-2}$ ($C_h = 2.3 \times 10^{-3}$ mJ/mol K^{-1}) with the small deviation to the T^{-2} fit around 0.15 K, which also appears in the direct plot as a deviation to $(C_h T^{-2} + \beta^* T^3)$ (dashed lines below 0.2 K), discussed in more details in the text.

with $\beta^* = 34$ mJ/mol K^4 and $C_h = 2.3 \times 10^{-3}$ mJ/mol K^{-1} , as shown in Figure 2. However, it can be seen that it remains a small positive deviation to this background between 0.1 and 0.2 K that we can attribute to a possible C_{LEE} contribution. The large dispersion of the data prevents to define a law for the temperature variation of this contribution, in particular a power law aT^ν , as was done for numerous DW compounds [4,5]. Nevertheless its amplitude is much less than for PF_6 samples [8,11]. We outline that the temperature where the deviation to the cubic regime occurs is the same one where the thermal transients start to deviate from an exponential decay (at $T = 0.25$ K); from our previous experiments on SDW or CDW compounds, that would indicate the appearance of the LEE contribution to C_p .

The first point to discuss is the origin of the hyperfine T^{-2} term. If we compare the C_h value obtained from

analysis (1) (C_h is much better determined in the T -range below 100 mK) to the values of C_h (or C_N) determined in the case of PF_6 , the present value is roughly 50 times smaller. Two different values were found in PF_6 ($C_N = 0.16$ and 0.065 mJ/molK $^{-1}$) for two different batches (Refs. [8,11] respectively), which we suppose to have different impurities content. A nuclear electric quadrupolar origin is not possible in the case of PF_6 since none of the constituent nuclei bears a quadrupolar moment (each of them has a nuclear spin $I = 1/2$). Such an origin could be possible in the case of AsF_6 (^{75}As has a spin $I = 3/2$), but the numerical comparison to PF_6 rules out this possibility, as well as the magnetic character of the electronic modulation.

The second possibility is the nuclear magnetism due to the local magnetic field H_{eff} induced by the SDW. We have previously outlined the numerical discrepancy for the local field estimation on the proton sites between the NMR data and the hyperfine specific heat data [23]: the specific heat yields over-estimated values for H_{eff} . In addition, we can also use the comparison with PF_6 to rule out this origin in both compounds. Supposing the same local field H_{eff} distribution in both of them, in particular on the anions AsF_6 and PF_6 (such an hypothesis is verified at the level of proton sites by ^1H -NMR, that is on the methyl groups [25,26]). The total amplitude of the magnetic nuclear specific heat is given, at the first order, by:

$$\frac{C_N}{R} = \frac{1}{3} \sum_i f_i \left(\frac{I+1}{I} \right) \left(\frac{\mu_\nu H_{eff}}{k_B T} \right)^2 \quad (2)$$

where the sum is extended to the different nuclei species, with f_i the atomic fraction of each species, I the nuclei spin, μ_ν the nuclear magnetic moment expressed in nuclear magneton μ_N and H_{eff} a mean local hyperfine field. For these two anions, the nuclei under consideration are ^{75}As ($I = 3/2$, $\mu_\nu = 1.4\mu_N$), ^{31}P ($I = 1/2$, $1.13\mu_N$) and ^{19}F ($I = 1/2$, $2.62\mu_N$), all with 100% of isotopic abundance. If one considers the total nuclei contribution to C_N from PF_6 and AsF_6 , one expects for a same H_{eff} a difference of less than 1% between the two compounds. In the extreme case where one considers only the contribution from As or P nuclei, the contribution to C_N from As is about 30% smaller than from P, contrary to the experimental results.

Consequently we now conclude that, at least for AsF_6 and PF_6 , the hyperfine T^{-2} term on short time scale does not have a nuclear hyperfine origin and can only be provided by the metastable LEE. Another argument for this common origin lies in an overall correlation between the amplitude of the residual contribution, which we usually named C_{LEE} , and that of the hyperfine term among AsF_6 and the two different PF_6 samples. In the present case, one can estimate, within the large experimental uncertainty (see inset of Fig. 2) a mean C_{LEE} contribution being about 0.03–0.05 mJ/molK at 0.15 K corresponding to $C_h = 2.3 \times 10^{-3}$ mJ/molK $^{-1}$. Similar tendency was obtained on the two PF_6 samples: C_h (previously quoted as C_N) = 0.16 mJ/molK $^{-1}$ with $C_{LEE}(T = 0.15 \text{ K}) \simeq 0.5$ mJ/molK from Refs. [11,23],

and $C_h = 0.065$ mJ/molK $^{-1}$ with $C_{LEE}(T = 0.15 \text{ K}) = 0.35$ mJ/molK from analysis of data reported in [8].

Generally the contribution beyond the regular lattice term (which we attribute now to the LEE of DW) can be decomposed into two different analytic expressions, each being dominant on different T -range and time scale: the power law T^ν ($\nu > 0$) obeyed on short-time scale and intermediate T -range, which progressively transforms in the T^{-2} tail of a Schottky anomaly at lower T . On increasing the experimental time scale, the Schottky tail progressively develops into a well-resolved Schottky contribution on the intermediate T -range: this was clearly shown in the case of PF_6 [8] where a Schottky anomaly is well-defined at sufficient long time, when the thermal equilibrium is reached (within 15–20 h). This was also observed in the case of Br compound [23], on a much smaller time scale than for PF_6 (within about 1h), and also in the present case as discussed in the following.

Finally, we ascribe the large difference in C_p defined on the short-time scale between PF_6 and AsF_6 below 0.5 K, as demonstrated in Figure 2, to the drastic reduction of LEE concentration for the latter compound. This could originate from a difference in the impurities content between the two compounds, in relation with different methods of synthesis [21].

3.2 The intermediate T^3 regime as a possible phason contribution

The most pronounced difference between AsF_6 and PF_6 clearly displayed in the Figure 1 occurs in the temperature range between 0.25 K and 1 K where the variation of C_p/T^3 is intermediate between two cubic regimes: the first one ascribed to the regular phononic part with a value of $\beta = 15$ mJ/molK 4 defined between 2 and 3 K, a value common to AsF_6 and PF_6 (see Fig. 1); the second one below 0.5 K with an amplitude β twice as large, such as $\beta^* \sim 34$ mJ/molK 4 . It should, however, be noted that in PF_6 the LEE contribution in this T -range is much larger than here, that can completely mask this intermediate regime.

One possibility for explaining the origin of these two plateaus in C_p/T^3 would be a change in the lattice contribution resulting from a phase transition towards another SDW sub-phase. However, if such a transition would actually exist, a characteristic C_p anomaly would have been detected and that was not the case.

A more plausible origin could be the contribution of the phason contribution. We have previously used this approach to analyze the broad bump in C_p/T^3 that we have measured in CDW systems, namely at 1.8 K in $(\text{TaSe}_4)_2\text{I}$ [24], 7 K in the platinum chain compound KCP [5] and 12 K in blue bronze [27].

¹ Usually in literature these two terms are supposed to be the manifestation of two different origins, C_N being from nuclei and $C_{LEE} \sim T^\nu$ from specific LEE, but in our case they are related to the same origin called LEE in the following.

Acoustic-like phason modes have been demonstrated in systems with incommensurate (IC) structures. They represent the sliding of the IC modulation wave recovering the broken translational high- T periodicity of the phase. Linear dispersions of the phason mode have been measured by inelastic neutron scattering in the CDW blue bronze compound [28], in the insulating IC ThBr₄ [29], in biphenyl [30], and in the incommensurate molecular compound of bis-(4-chlorophenyl) sulphone BCPS [31]. For the last compound [32] and biphenyl [33] the analysis of the specific heat data has shown the contribution of the phason mode. Impurities and high order commensurability effects may produce a locking of the modulation wave to the underlying lattice and introduce a gap ω_0 in the phason spectrum:

$$\omega_q^2 = \omega_0^2 + k^2(q - q_0)^2$$

where q_0 is the wave vector of the IC distortion.

Following Boriack and Overhauser [34] the analysis of the phason contribution to the specific heat of a CDW system consists of a modified Debye-like spectrum with two cut-off frequencies: the lower one corresponding to the phason gap given by the CDW pinning frequency ω_0 , and the upper one is the phonon frequency ω_φ at q_0 in the absence of the modulation. We were able to fit the bump in C_p/T^3 for the three CDW compounds [5, 24, 27] with reasonable parameters, in particular with ω_0 values obtained from microwave or far-infrared measurements.

However, this phason approach has been shown to be questionable in these CDW cases and a more simple interpretation was recently given [35]. It is based on a lattice phonon origin due to the specific character of the phonon branches in these quasi one-dimensional compounds. Thus, it was shown that in these three compounds the bump in C_p/T^3 can be obtained from calculations of the phonon density of states derived from the low energy phonon branches, especially low optic modes with no (or a small) dispersion in the Brillouin zone and flat sections of acoustic branches near the Brillouin zone boundary. The case of (TaSe₄)₂I is the most unusual due to non-dispersive transverse acoustic modes in more than half the Brillouin zone at a frequency of 150–200 GHz, depending on the TA mode.

If, as in the case of CDWs, one would like to analyze the jump in C/T^3 around 0.5 K in AsF₆ as a contribution of phonon modes (and more likely to transverse acoustic modes), one would be led to estimate the frequency of these phonon modes to be in the range of a few GHz. Assuming a sinusoidal dispersion, one would get a sound velocity at $q \rightarrow 0$ of a few dozen of m/s, which seems unreasonable.

Thus, after having ruled out a phonon origin, let us consider a possible contribution of phasons for explaining this C_p variation. We will use a similar treatment for SDW and CDW concerning the phason contribution to C_p . Phase excitations for the SDW result in charge fluctuations. As longitudinal deformations of the SDW phase yield charge redistribution, they involve long range Coulomb interaction; when these Coulomb forces are not

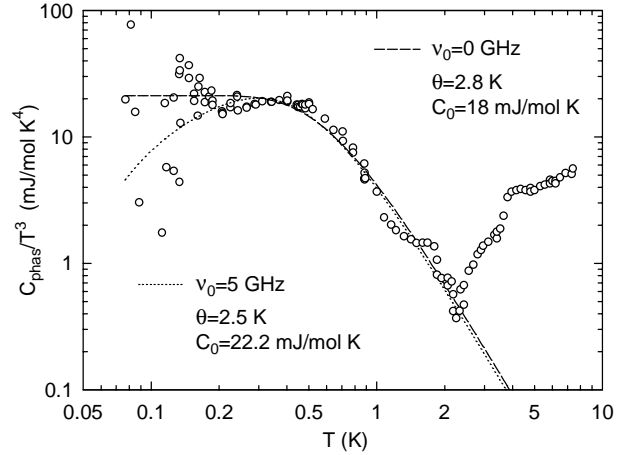


Fig. 3. Residual specific heat of AsF₆, in C/T^3 , after subtraction of the regular phonon contribution ($\beta = 14.9$ mJ/mol K⁴) and the LEE contribution determined as in Figure 2 (inset), ascribed to the phason modes. The fit to the data is given by the Debye-like model (see formula (3)) for the phason excitations, with two possible values ($\nu_0 = 0$ or 5 GHz) for the lower cut-off frequency (pinning frequency), an upper cut-off of 50–60 GHz (corresponding temperature $\theta \simeq 2.5$ –2.8 K) and with $C_0 = 3N_\phi k_B$.

screened, which is the case in the low temperature insulating state of AsF₆, the longitudinal phason mode is raised to the plasma frequency above the SDW gap [36] whereas the transverse phason modes are expected to be unaffected. Nevertheless, we use for the excitation spectrum a modified Debye model with only one branch with two cut-off frequencies. The lower one corresponds to the phason gap given by the pinning frequency ν_0 and the upper one is the “phason Debye frequency”, $\nu_\varphi = k_B\theta_\varphi/h$, which in the SDW case can be the amplitude mode frequency [34]

$$C_\varphi = 3N_\phi k_B \left(\frac{T}{\theta_\varphi}\right)^3 \int_{T_0/T}^{\theta_\varphi/T} (x - x_0)^2 \frac{x^2 e^x}{(e^x - 1)^2} dx \quad (3)$$

with $x = h\nu/k_B T$ and N_ϕ the number of phason mode excitations. A low frequency resonance has been found in PF₆ [37] in microwave experiments with $\nu_0 = 5$ –6 GHz at $T = 2$ K which has been ascribed to the collective response of the pinned SDW [38].

In the absence of pinned mode ($\nu_0 = 0$), the phason contribution to C_p should appear as a step in excess to the phonon contribution in the C/T^3 versus T plot. With a finite ν_0 , due to the lower cut-off in equation (3) the low temperature contribution to C_p is suppressed and the overall phason contribution appears as a bump. In Figure 3 we have drawn the temperature variation of the residual specific heat of AsF₆ after subtraction of the phonon contribution $15 T^3$, the LEE contribution defined as in Figure 2 (see the inset). The dashed line in Figure 3 corresponds to the phase mode contribution with $\nu_0 = 0$ and $\nu_\varphi = 60$ GHz = 2.8 K. The dotted line corresponds to the case of a pinned mode $\nu_0 = 5$ GHz.

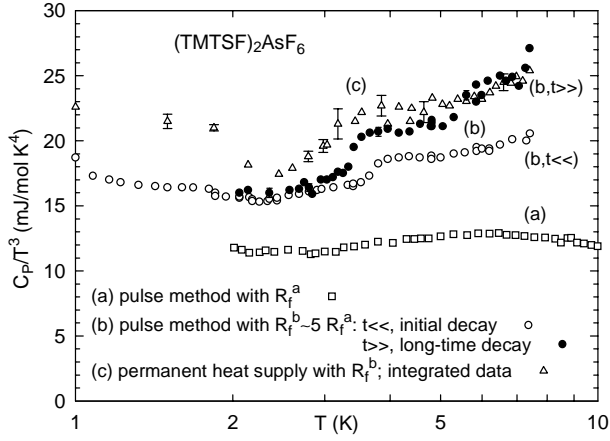


Fig. 4. Specific heat data in C_p/T^3 between 1 and 10 K, collected on the same AsF_6 sample, with two different transient heat-pulse techniques which correspond to two different sample arrangements (with two different heat links R_f). Measured values of C_p/T^3 increase with the growth of the transient time-constant τ , and/or with the duration of the heat pulse. First experimental arrangement (a) with R_f^a and the shortest τ gives the lowest results ([39] \square). Second arrangement (b) was with $R_f^b \simeq 5R_f^a$. Different analyses of the same thermal transient for shorter pulses (less than 1 s) give smaller values on short time scale (\circ), than on long-time exponential decay (\bullet) (see Fig. 5). Integrated total heat release for very long pulses (about 100–300 s) yields the largest values (\triangle).

4 Lattice and configurational contributions: the anomalies at 1.9–2.0 K and 3.5 K

In the T -range between 1 and 7 K (Fig. 1), C_p deviates slightly from a general cubic variation, but shows successively at 1.9–2.0 K and 3.5 K two smooth anomalies. This behavior is quite similar to that of PF_6 [11], but with important differences concerning the anomaly at 3.5 K. Indeed, in PF_6 we have observed a well-defined jump with a characteristic hysteretic behavior in the vicinity of 3.5 K, in relation with a strong dependence on previous thermal history, which enables us to ascribe this transition to a glassy-like transition [12]. In the case of AsF_6 we could not detect similar effects, such as the spontaneous evolution of C_p during a long isothermal stabilization. However, the metastable character of the system is manifested also, as in PF_6 , by the dependence of the specific heat upon the dynamical conditions of the experiments. In Figure 4 are reported three series of data collected on the same sample ($m \simeq 90$ mg), using two different transient-heat pulse techniques on two different cryostats and sample arrangements:

- The data (a) were obtained on a He^4 cryostat [39], with a sample holder more strongly connected to the cold sink (R_f about 5 times smaller) than in the present arrangement, which resulted in kinetics of the transients three times more rapid. In addition, below 5 K the duration of the heat pulses was about 2 times smaller than presently;

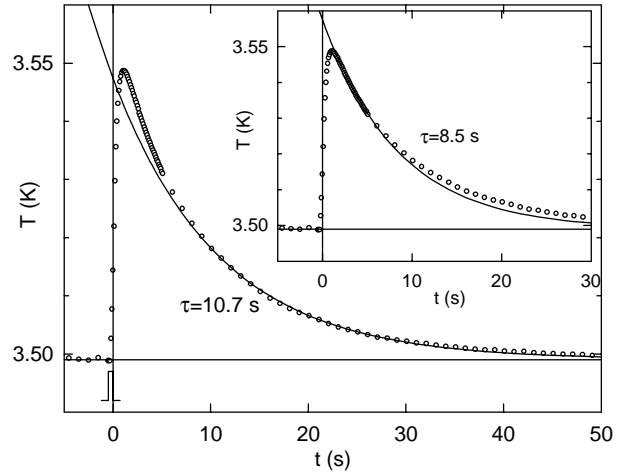


Fig. 5. The decay of the temperature increment $\Delta T(t)$ in $(\text{TMTSF})_2\text{AsF}_6$ at 3.52 K after a heat pulse of 0.5 s, and the two possible analyses of the transient. The main figure shows the determination of C_p (data \bullet in Fig. 4) from the exponential decay ($\tau = 10.7$ s) obeyed about 5 s after the heat pulse. In the inset, we show the determination of C_p (data \circ in Fig. 4) from the initial part of the decay (a possible exponential with $\tau = 8.5$ s). For $T < 3$ K down to about 0.25 K, the slight deviation to an exact exponential transient disappears, and the two determinations, at initial and long times, yield similar C_p values.

- Data (b) and (c) were obtained with the present experimental arrangement in another cryostat, the only difference concerns the duration of heat delivery. Whereas (b) are obtained with pulses of duration from 0.2 to 1 s between 1 and 7 K, data (c) are obtained with heat duration varying between 100 and 300 s. Some data are obtained with duration of 10 minutes.

As a general result, the heat capacity systematically increases when the experimental time-span increases (either the dynamics of the transients, or the duration of pulses). However, these effects are of much less amplitude than for those measured below 0.3 K, where one measures an increase by at least a factor of 10 when the heat supply duration (or “waiting time”) increases from pulse of 0.2 s to 600 s. As well, within conditions (b), the precise analysis of the transient shows a change of regime starting around 3 K: whereas below this temperature the transients are well-analyzed with a unique exponential, above it they are characterized by two successive exponentials with slightly different (20–30%) time constants (demonstrated in Fig. 5). The C_p data obtained from the second time constant over a time-span of a few tens seconds (full circle \bullet in Fig. 4) are larger than those from the initial decay (open circle \circ), so that the knee at 3.5 K, interpreted as a glass transition in the case of PF_6 , appears to be sensitive to the experimental kinetics. Whereas it is well-defined for data (b), particularly on long time-span, and (c), it is washed out for data (a) where only remains a shallow bump centered at 7 K. This bump is a common feature to the $(\text{TMTSF})_2\text{X}$, $\text{X} = \text{AsF}_6$ and

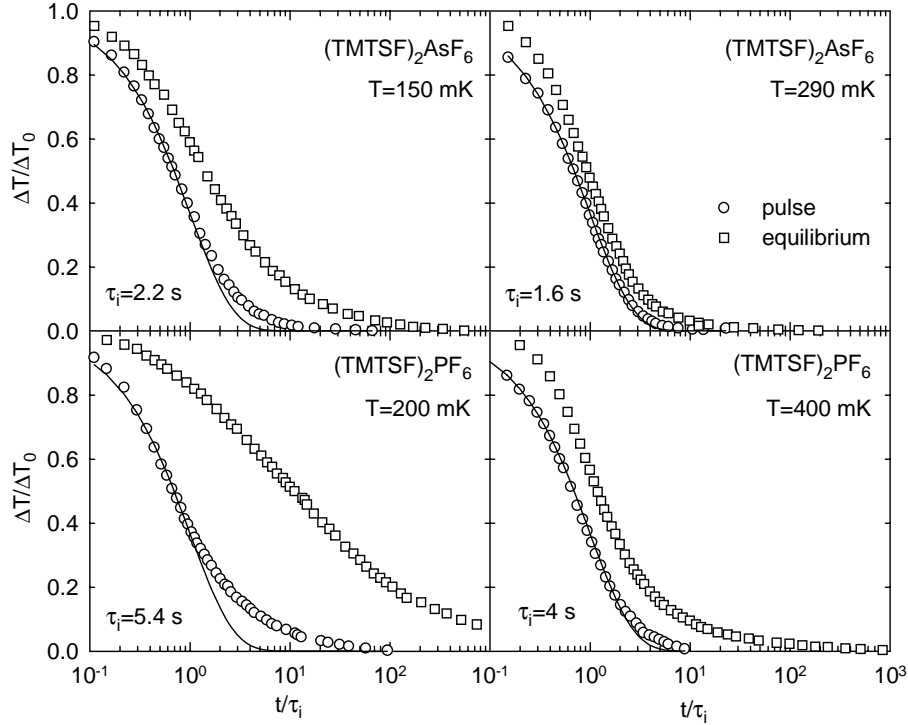


Fig. 6. Heat transients $\Delta T/\Delta T_0$ as a function of normalized time, t/τ_i , for short pulses (\circ) and for the permanent heat supply when the system reaches thermodynamic equilibrium (\square) compared for AsF_6 and PF_6 (the same batch as in Ref. [8]) at different temperatures. τ_i is the time constant of the initial part of the response to the short pulse. The corresponding exponentials are shown by the full lines. Aging in AsF_6 can be detected at 290 mK and it develops at lower T , but the intensity of the effect at 150 mK is much smaller than for PF_6 at 200 mK and corresponds to that one for PF_6 at approximately 400 mK.

PF_6 , and $(\text{TMTTF})_2\text{Br}$ salts which can be ascribed to low-frequency soft lattice modes [39].

These time-dependence effects are generally related to the presence of configurational excitations in addition to the regular phonon term. This configurational contribution can follow a T^3 variation (see Fig. 2 in Ref. [40] for PF_6), with an amplitude which can be similar to that of the vibrational excitations (data (c) *vs.* data (a) for AsF_6) This property allows us to define a baseline in C/T^3 which we call “regular phonon background”, as explained in Figure 1.

All these data taken together show that the jump, characteristic of the glassy transition in the sense of the freezing-in of the configurational degrees of freedom, can be observed only within a limited time-span range, which corresponds to the relaxation of the excitations within this time-span [41].

The overall increase of C/T^3 values, with a similar amplitude, was observed on the three organic SDW compounds we have investigated: PF_6 , Br, and AsF_6 . On the contrary, it was absent in the case of metallic phase (relaxed state) of ClO_4 , with a ground state which is superconductor at $T_c = 1.2$ K [42].

5 Long time heat relaxation

It was shown in Figures 1 and 2 that C_p deviates from a T^3 law with decreasing temperature due to the presence of the additional contribution of LEE’s. This deviation occurs in AsF_6 below 0.2 K, simultaneously with the occurrence of non-exponential kinetics. In the same temperature range, the energy relaxation shows a strong dependence on the duration of the heat flow that we call “waiting time” as shown in Figure 6. In the case of PF_6 , the C_{LEE} contribution starts to be dominant over the phonon contribution below $T^* \simeq 0.4\text{--}0.5$ K [8, 23]. Although the regular phonon contribution in both materials (PF_6 and AsF_6) is very similar (see Fig. 2), due to the fact that the C_{LEE} contribution is more than one order of magnitude smaller in AsF_6 , the pronounced time dependence occurs at a much lower T^* ($T^* = 0.1\text{--}0.15$ K) in AsF_6 with respect to PF_6 .

5.1 Aging effect

In order to compare the magnitude of the time dependence in AsF_6 and PF_6 compounds, we have renormalized the time scale of the temperature decay in Figure 5 (transient $\Delta T(t)$) with the time constant τ_i of the initial part of the response to the shortest pulses (in the order of 2 s in this T -range). As noticed in Section 2, the experimental conditions for the thermal link are rather similar

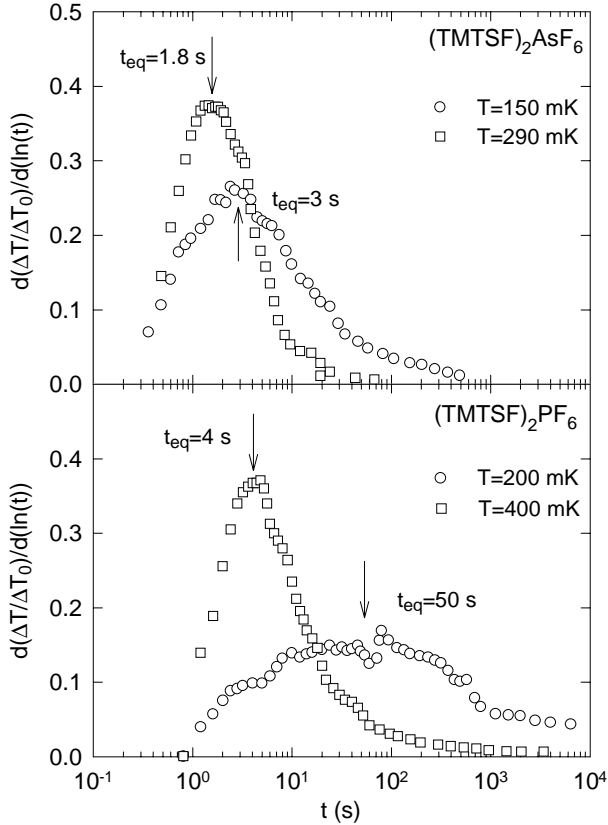


Fig. 7. The relaxation rates $d(\Delta T(t)/\Delta T_0)/d(\log t)$ as a function of time in the thermodynamic equilibrium for AsF₆ and PF₆ for temperatures as in Figure 6. Aging is much more pronounced for PF₆: equilibrium times t_{eq} (the position of the maximum) moves more to longer time and the distribution of relaxation times broadens significantly.

for the present AsF₆ experiment and for PF₆ [8] (more details in captions of Figs. 6 and 7).

The effect of time dependence (out of equilibrium phenomenon) named *aging* (due to similarities with spin glasses and polymers [43], explained in details in Ref. [44]) starts to be effective below 0.5 K in PF₆ and observable below 0.25 K in AsF₆.

We have found for AsF₆ all the characteristic features that we have already investigated in other density wave systems, especially well defined in PF₆ [8] and in the CDW compound TaS₃ [45]. Figure 6 shows the thermal transients $\Delta T(t)$ of AsF₆ and of PF₆ for comparison for different durations of the heat supply at two different temperatures.

- Aging manifests itself in the way that the energy relaxation after the heat pulse occurs at longer time when the duration of the pulse is longer (see the difference for short pulses of seconds and long energy supply of minutes or hours in Fig. 6).
- Saturation of aging, when the system reaches thermodynamic equilibrium, is realized in AsF₆ within much shorter time than in PF₆.
- The excitation spectrum $g(\tau)$ which is proportional to the logarithmic derivative of the transient

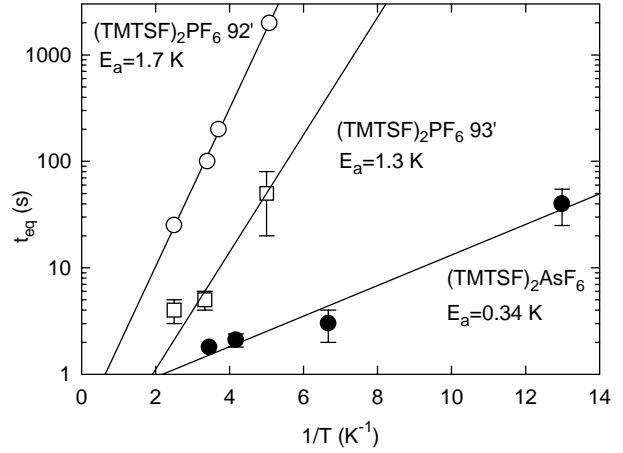


Fig. 8. Arrhenius plot of the equilibrium relaxation time t_{eq} demonstrates the activated behaviour of underlined processes in AsF₆ and PF₆. 4–5 times larger activation energy for PF₆ [8,7] is the reason that instead of few seconds for AsF₆ in the range 150–200 mK, one has to go over the reasonable experimental time of 1000 s, and wait even for days at 100 mK.

$\partial \Delta T(t)/\partial \log t$ broadens when T is decreased, extending on several decades. This is represented in Figure 7 for equilibrium waiting times (the time of 10 min necessary for probing the whole distribution of relaxation times) at $T = 0.29$ and 0.15 K. One defines the equilibrium relaxation time, t_{eq} , as the position of the maximum in $g(\tau)$ when aging is saturated.

From Figures 6 and 7 it can be seen that at $T = 0.15$ K for an energy supply of 10 min, AsF₆ is already in the thermodynamic equilibrium, while in PF₆ at $T = 0.2$ K one has to pump heat into the system at least one hour in order to probe the complete LEE spectrum. It evolves even during weeks at slightly lower T .

Processes responsible for a so long relaxation in both systems are thermally activated ($\tau = \tau_0 e^{E_a/kT}$). The main difference between AsF₆ and PF₆ appears in the magnitude of the activation energy, as shown in Figure 8 where we have plotted $\log t_{eq}$ versus $1/T$. The attempt microscopic time for the Arrhenius behaviour, τ_0 , is very close for both systems: $\tau_0 = 0.3$ –1 s; but the corresponding activation energies are very different: $E_a \simeq 1.7$ K or 1.3 K for PF₆ ([7] and [8] respectively), whereas $E_a \simeq 0.35$ K for AsF₆.

Out of equilibrium phenomena are directly related to the character of the phase space. The cross-over from a non-equilibrium to an equilibrium regime in the aging phenomena observed in our experiments has been named “interrupted aging” by Bouchaud in his phenomenological model on weak ergodicity breaking and aging in disordered systems [46]. It is possible within this model to estimate the number of metastable states in a complex system when the exploration of the phase space is completed, *i.e.* the aging has stopped. The ergodic time t_{eq} corresponds to the time for which all accessible metastable states behind the energy barriers in the corrugated phase space have been visited and consequently it is a measure of

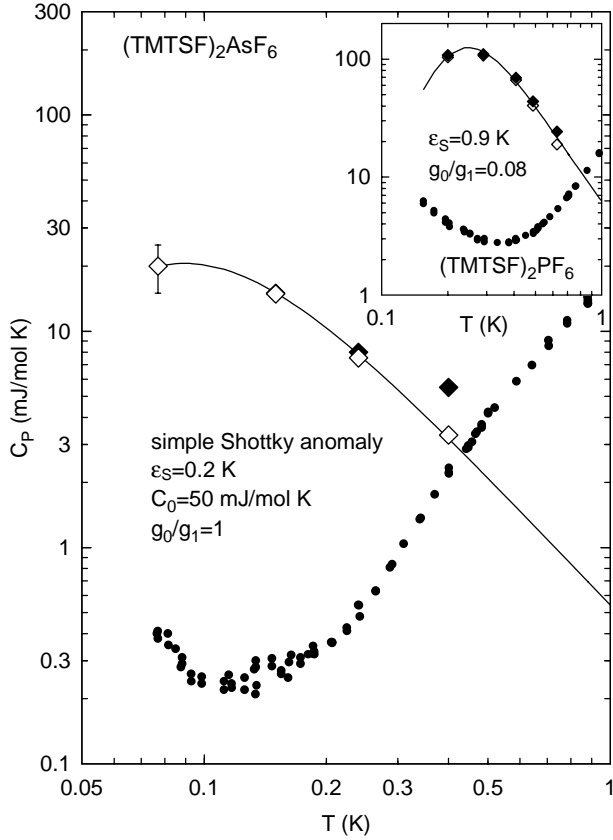


Fig. 9. Specific heat of AsF_6 in thermodynamical equilibrium obtained by total integration (\blacklozenge) compared to the short-time C_p . The anomaly which remains after subtraction of the short time C_p (\diamond) can be fitted to the Schottky anomaly (full line) with the corresponding parameters given in the figure. Inset shows similar anomaly for PF_6 .

the “complexity” of the system. Larger barrier height in PF_6 and similar attempt microscopic times $\tau_0 \sim 1$ s force this system to experience ergodicity breaking at higher T than in AsF_6 . The “complexity” of the system is defined as $\Omega \propto \log t_{eq}/\log \tau_0$; it reaches high values of order 20 in spin glasses [46] assuming a microscopic time $\tau_0_{SG} \sim 10^{-9}$ s. In the present SDW case, from the activated nature of the underlined relaxational process, the classification is simply related to the ratio of the corresponding activation energies what implies that the “complexity” of PF_6 is 5 times larger than for AsF_6 at the same T .

5.2 C_p in thermodynamical equilibrium: Schottky anomaly

As it was shown in details in [8], the heat capacity in conditions of thermal equilibrium, C_{peq} (when aging is saturated) determined from the integration of the total energy release is strongly different from the short time C_p . That is demonstrated in Figure 9 for AsF_6 . Below $T = 0.5$ K, C_{peq} increases with decreasing T and reaches a maximum between 0.08 K and 0.150 K. This tem-

perature dependence of C_{peq} has all the characteristics of a Schottky anomaly with a great similarity to that obtained in PF_6 [8, 23] as shown in the inset for comparison. Scaling between the corresponding physical parameters can be obtained by a simple translation in the log-log plot. The Schottky anomaly in PF_6 yields the splitting energy $\epsilon_s = 0.9$ K, $C_{peq,max} = 120$ mJ/molK at $T_{max} = 0.25$ K and with a relatively large ratio of degeneracy $g_1/g_0 \simeq 12$.

For AsF_6 , the parameters of the Schottky anomaly are: $C_{peq,max} = 20$ mJ/molK, $T_{max} = 0.08$ K, the splitting energy $\epsilon_s \simeq 0.2$ K and almost no degeneracy. Thus, the corresponding ratios between energy barriers E_a and splitting energies ϵ_s are 1.9 or 1.4 for PF_6 and 1.75 for AsF_6 . This gives a new information concerning the relative roughness of the phase space for both systems. There is a self-similarity in phase space as demonstrated by the close ratios between the height of the largest barrier in the system and the relative energy difference between the levels of various metastable states. However, at the same observation temperature, PF_6 has certainly a more rough free energy landscape and consequently it exhibits a more pronounced disordered ground state.

It was recently proposed that strong pinning centers close to regions of commensurability can give rise to plastic deformation of the density wave with many metastable states with long relaxation time between them [47]. The contribution of LEE’s to the specific heat was shown to depend on the “pumping time” and to show a Schottky anomaly behaviour.

6 Conclusions

Our low-temperature thermodynamical investigations in the SDW ground state of $(\text{TMTSF})_2\text{AsF}_6$ have shown remarkable features. It appears that the discontinuities in the lattice contribution at 1.9 K and 3.5 K are a common feature in the Bechgaard salts as also manifested in many other physical properties; whereas in $(\text{TMTSF})_2\text{PF}_6$ we have observed a well-defined jump in C/T^3 at 3.5 K with a hysteretic behaviour that we have ascribed to a glassy-like transition, no such hysteresis was measured in $(\text{TMTSF})_2\text{AsF}_6$. However metastability in this T -range is manifested by the dependence of the specific heat on the dynamical conditions of the experiments.

Below 0.5 K the measured specific heat exhibits all features previously found for DW systems. Moreover, we have demonstrated that the hyperfine T^{-2} term cannot have a nuclear hyperfine origin but should be provided by the metastable LEE excitations. They relax through the thermally activated process with a very broad distribution of relaxation times. On increasing the experimental time during which the heat is poured into more and more low-energy modes of the SDW (pumping time or waiting time) this tail progressively develops into a well-resolved Schottky contribution. However, a specific character of the $(\text{TMTSF})_2\text{AsF}_6$ sample we have measured is the drastic reduction of the LEE concentration with respect to $(\text{TMTSF})_2\text{PF}_6$, which could originate from a different impurity content in these the two compounds.

This reduction of the LEE is the manifestation of a less disordered SDW ground state, with the consequence of a smaller thermal activation energy for the equilibrium dynamics and a smaller “complexity” parameter (as defined in [46]) of the phase space. On the other hand, consequently to this reduction of the LEE contribution, an intermediate cubic-like regime is detected between 0.25 and 0.5 K. We have analyzed this behaviour as the SDW phason contribution with a phason gap of a few GHz in agreement with microwave experiments. In the case of PF₆ salt, this contribution was masked by the larger LEE contribution. Measurements on (TMTSF)₂AsF₆ crystals in which a controlled amount of defects are introduced are planned in order to more specifically relate the amplitude of the LEE contribution and of their dynamics with the introduced defects.

References

1. D. Jérôme, H.J. Schulz, *Adv. Phys.* **31**, 299 (1982); T. Ishiguro, K. Yamaji, *Organic superconductors* (Springer-Verlag, Berlin, 1990); G. Grüner, *Rev. Mod. Phys.* **66**, 1 (1994).
2. T. Takahashi, Y. Maniwa, H. Kawamura, G. Saito, *J. Phys. Soc. Jpn* **55**, 1367 (1986).
3. S. Tomić, J.R. Cooper, D. Jérôme, K. Bechgaard, *Phys. Rev. Lett.* **62**, 462 (1989); T. Sambongi, K. Nomura, T. Shimizu, K. Ichimura, N. Kinoshita, M. Tokomoto, H. Anzai, *Solid State Commun.* **72**, 817 (1989); W. Kang, S. Tomić, J.R. Cooper, D. Jérôme, *Phys. Rev. B* **41**, 4862 (1990).
4. J.C. Lasjaunias, K. Biljaković, P. Monceau, *Physica B* **165-166**, 893 (1990).
5. J. Odin, J.C. Lasjaunias, A. Berton, P. Monceau, K. Biljaković, *Phys. Rev. B* **46**, 1326 (1992).
6. K. Biljaković, J.C. Lasjaunias, P. Monceau, F. Levy, *Phys. Rev. Lett.* **62**, 1512 (1989).
7. K. Biljaković, F. Nad', J.C. Lasjaunias, P. Monceau, K. Bechgaard, *J. Phys.-Cond.* **6**, L135 (1994).
8. J.C. Lasjaunias, K. Biljaković, P. Monceau, *Phys. Rev. B* **53**, 7699 (1996).
9. T. Takahashi, T. Harada, Y. Kobayashi, K. Kanoda, K. Suzuki, K. Murata, G. Saito, *Synth. Met.* **41-43**, 3985 (1991).
10. K. Nomura, Y. Hosokawa, N. Matsunaga, T. Sambongi, H. Anzai, *Synth. Met.* **70**, 1295 (1995).
11. J.C. Lasjaunias, K. Biljaković, P. Monceau, K. Bechgaard, *Solid State Commun.* **84**, 297 (1992).
12. J.C. Lasjaunias, K. Biljaković, F. Nad', P. Monceau, K. Bechgaard, *Phys. Rev. Lett.* **72**, 1283 (1994).
13. J.P. Pouget, S. Ravy, *J. Phys. I France* **6**, 1501 (1996); *Synth. Met.* **85**, 1523 (1997).
14. F. Nad', P. Monceau, K. Bechgaard, *Solid State Commun.* **95**, 655 (1995).
15. J.L. Musfeldt, M. Poirier, P. Batail, C. Lenoir, a) *Phys. Rev. B* **51**, 8347 (1995); b) *Phys. Rev. B* **52**, 15983 (1995).
16. S. Uji, J.S. Brooks, M. Chaparala, S. Takasaki, J. Yamada, H. Anzai, *Phys. Rev. B* **55**, 12446 (1997).
17. J.S. Brooks, R.G. Clark, R.H. McKenzie, R. Newbury, R.P. Starrett, A.V. Skougarevski, M. Tokumoto, S. Takasaki, J. Yamada, H. Anzai, S. Uji, *Phys. Rev. B* **53**, 14406 (1996).
18. J.P. Ulmet, A. Narjis, M.J. Naughton, J.M. Fabre, *Phys. Rev. B* **55**, 3024 (1997).
19. M. Nagasawa, T. Sambongi, K. Nomura, H. Anzai, *Solid State Commun.* **93**, 33 (1995).
20. G. Kriza, G. Quirion, O. Traetteberg, D. Jérôme, *Europhys. Lett.* **16**, 585 (1991).
21. It was however noted in reference [19] that quality of crystals from the same source of (TMTSF)₂AsF₆ is much superior to that of (TMTSF)₂PF₆.
22. K. Biljaković, J.C. Lasjaunias, P. Monceau, F. Levy, *Europhys. Lett.* **8**, 771 (1989).
23. J.C. Lasjaunias, P. Monceau, D. Starešinić, K. Biljaković, J.M. Fabre, *J. Phys. I France* **7**, 1417 (1997).
24. K. Biljaković, J.C. Lasjaunias, F. Zougmore, P. Monceau, F. Levy, L. Bernard, R. Currat, *Phys. Rev. Lett.* **57**, 1907 (1986).
25. M.F. Hanson, Ph.D. dissertation, Los Angeles, University of California (1994), Figs. 3–4, unpublished.
26. W.G. Clark *et al.*, *Synth. Met.* **85**, 1941 (1997).
27. J. Odin, K. Biljaković, K. Hasselbach, J.C. Lasjaunias (to be published).
28. J.P. Pouget, B. Hennion, C. Escribe-Filippini, M. Sato, *Phys. Rev. B* **43**, 8421 (1991); B. Hennion, J.P. Pouget, M. Sato, *Phys. Rev. Lett.* **68**, 2374 (1992).
29. L. Bernard, R. Currat, P. Delamoye, C.M.E. Zeyen, S. Hubert, R. de Kouchkovsky, *J. Phys. C. Solid State Phys.* **16**, 433 (1983).
30. P. Launois, F. Moussa, M.H. Lemée-Cailleau, H. Cailleau, *Phys. Rev. B* **40**, 5042 (1989).
31. J. Ollivier *et al.*, *Phys. Rev. Lett.* **81**, 3667 (1998).
32. J. Etrillard, J.C. Lasjaunias, K. Biljaković, B. Toudic, G. Coddens, *Phys. Rev. Lett.* **76**, 2334 (1996).
33. J. Etrillard, J.C. Lasjaunias, B. Toudic, H. Cailleau, *Europhys. Lett.* **38**, 347 (1997).
34. M.L. Boriack, A.W. Overhauser, *Phys. Rev. B* **18**, 6454 (1978).
35. H. Requardt, R. Currat, P. Monceau, J.F. Lorenzo, A.J. Dianoux, J.C. Lasjaunias, J. Marcus, *J. Phys.-Cond.* **9**, 8639 (1997).
36. K. Maki, G. Grüner, *Phys. Rev. Lett.* **66**, 782 (1991).
37. S. Donovan, Y. Kim, L. Degiorgi, G. Grüner, *J. Phys. I France* **3**, 1493 (1993); S. Donovan, Y. Kim, L. Degiorgi, M. Dussel, G. Grüner, W. Wonenberger, *Phys. Rev. B* **49**, 3363 (1994).
38. We suppose that the pinned mode for AsF₆ appears at the same frequencies as for PF₆ [37].
39. H. Yang, J.C. Lasjaunias, P. Monceau, *Phys. Rev. B* (submitted).
40. J. Odin, J.C. Lasjaunias, K. Biljaković, P. Monceau, K. Bechgaard, *Solid State Commun.* **91**, 523 (1994).
41. J.C. Lasjaunias, J. Odin, K. Biljaković, P. Monceau, K. Bechgaard, *ECRYS 93, J. Phys. IV Colloq. France* **3**, C2-365 (1993).
42. H. Yang, J.C. Lasjaunias, P. Monceau (to be published).
43. Ph. Refrigier, E. Vincent, J. Hamman, M. Ocio, *J. Phys. France* **48**, 1533 (1987).
44. K. Biljaković, J.C. Lasjaunias, P. Monceau, *ECRYS 93, J. Phys. IV Colloq. France* **3**, C2-335 (1993).
45. K. Biljaković, J.C. Lasjaunias, P. Monceau, P. Levy, *Phys. Rev. Lett.* **67**, 1902 (1991).
46. J.P. Bouchaud, *J. Phys. I France* **2**, 1705 (1992).
47. Yu.N. Ovchinnikov, K. Biljaković, J.C. Lasjaunias, P. Monceau, *Europhys. Lett.* **34**, 645 (1996).